HIF-1α, NOTCH1, ADAM12, and HB-EGF are overexpressed in mucoepidermoid carcinoma

Dimitra Castelo Branco, DDS, MSc, Natacha Malu Miranda da Costa, DDS, MSc, Caio Tadashi Saab Abe, Maria Sueli da Silva Kataoka, DDS, MSc, PhD, João de Jesus Viana Pinheiro, DDS, MSc, PhD, and Sérgio de Melo Alves Júnior, DDS, MSc, PhD

Objective. Intratumoral hypoxia (IH) occurs during cellular proliferation of malignant tumors. This phenomenon is characterized by a decrease in oxygen levels in the neoplastic microenvironment. Throughout this condition, the proteins HIF-1α, NOTCH1, ADAM12, and HB-EGF can be activated, triggering signaling pathways associated with tumor invasiveness through invadopodia formation. This study aimed to evaluate the immunostaining of HIF-1α, NOTCH1, ADAM12, and HBEGF in 19 cases of mucoepidermoid carcinoma (MEC) and 10 samples of salivary glands (control group).

Study Design. The immunoperoxidase technique was employed to detect the proteins of interest. The Student *t* test was used to compare immunoexpression between MEC samples and the control group.

Results. Protein immunostaining was statistically significantly higher in MEC samples than in the control group ($P < .01$), and the proteins were especially overexpressed in epidermoid cells of MEC.

Conclusions. We suggest that there is an association between the NOTCH1 signaling pathway activated by IH and the biologic behavior of MEC. (Oral Surg Oral Med Oral Pathol Oral Radiol 2019;127:e8−e17)

Mucoepidermoid carcinoma (MEC) is the most common malignant neoplasm of the salivary glands, representing about 30% of all malignant tumors in that region.[1,2] Clinically, it is a slow-growing mass, most often located in the parotid gland and has high rates of local recurrence and metastasis.[3] Histologically, MEC is composed of 3 cell populations: mucous, intermediate, and epidermoid.[3-6] These cells can be organized into cystic, solid, or infiltrative growth patterns.[3-6]

Malignant tumors of the salivary glands, in particular MEC, have been associated with lower sensitivity to therapy because of their capacity for invasion and metastasis formation.[7,8] Acute hypoxia is the limited perfusion and temporary reduction of the oxygen (O_2) supply in the tumor microenvironment. However, chronic hypoxia results from insufficient vascularization and limitation of O_2 diffusion during tumor growth.[9,10] Neoplastic invasion is related to intratumoral hypoxia (IH). Clinically, IH is related to poorer prognosis, especially in head and neck cancer.[11,12] Moreover, evidence shows that acute hypoxia in neoplastic cells contributes to tumoral progression.[9-14]

Under hypoxic conditions, tumor cells can develop compensatory mechanisms that contribute to cellular proliferation, such as angiogenesis, changes in cellular metabolism, and activation of proteins and transcription factors involved in the processes of invasion and metastasis.[11,12]

Permanent alterations in neoplastic cells under IH conditions are regulated mainly by hypoxia-inducible factor-1α (HIF-1 α).[15,16] HIF-1α is a transcription factor that regulates the hypoxia responsive elements, which regulate homeostasis of systemic and cellular oxygen O_2[9,15]; it is also associated with transcription of genes and activation of proteins and growth factors involved in cellular development.[16-18] There is an important role for HIF-1α in the stabilization of intracellular responses triggered by Notch homolog 1, translocation-associated-Drosophila (NOTCH1) via Jagged 2.[15,19,20]

The NOTCH1 signaling pathway may be activated in a cell contact−dependent interaction via receptor-ligand binding (NOTCH1-Jagged 2). Under hypoxia conditions, NOTCH1 is associated with activation of growth factors and transcription of genes,[19,20] such as A disintegrin and metalloprotease 12 (ADAM12).[15,21]

ADAM12 is a metalloprotease belonging to the adamalysin family, and it is overexpressed in many

Statement of Clinical Relevance

Mucoepidermoid carcinoma overexpresses HIF-1α, NOTCH1, ADAM12, and HBEGF. Stabilization of HIF-1α under tumor hypoxia may increase the activity of the NOTCH signaling pathway and raise ADAM12 activity, which could contribute to invadopodia formation and tumor metastasis.

Coordination of Improvement of Higher Education Personnel (CAPES) provided the funding for this study.

Department of Oral Pathology, School of Dentistry, Federal University of Pará-UFPA, Belém, Brazil.

Received for publication May 11, 2018; returned for revision Sep 14, 2018; accepted for publication Sep 23, 2018.

2212-4403/$-see front matter
http://doi.org/10.1016/j.oooo.2018.09.013

Table I. Distribution of 19 mucoepidermoid carcinoma (MEC) cases according to demographic, lifestyle, and clinicopathologic variables

	Cases	
Variables	*N*	*%*
Age (years)		
<31	4	21
31–40	4	21
45–50	2	10.5
51–60	4	21
61–70	2	10.5
71–80	2	10.5
81–90	1	5.5
Gender		
Male	9	47.36
Female	10	52.64
Race		
Caucasian	11	57.90
Non-Caucasian	8	42.10
Alcohol Consumption		
Yes	9	47.37
No	10	52.63
Smoking Habit		
Yes	6	31.60
No	13	68.40
Clinical Stage		
Stage I–II	9	47.36
Stage III–IV	10	52.64
Histopathologic Grading		
I	14	73.68
II	0	0
III	5	26.32
Site		
Palate	7	36.84
Parotid gland	10	52.64
Submandibular gland	2	10.52
Actual State		
Alive	16	84.21
Not alive	3	15.79

carcinoma types.[22] ADAM12 activation allows the shedding of growth factors from their ectodomains located at the cellular membrane, such as heparin-binding endothelial growth factor–like growth factor (HB-EGF).[20,23]

HB-EGF is a ligand of epidermal growth factor receptor (EGFR). The membrane-anchored HB-EGF (pro-HB-EGF) is cleaved on the cell surface by ADAM12, and the soluble form (HB-EGF-s) is released. Overexpression of HB-EGF-s is found in malignant neoplasms and is related to the mechanisms of invadopodia formation, pathologic cell proliferation, and metastasis.[23,24]

In view of the relationship between the hypoxia signaling pathway and malignant tumor progression, we aimed to analyze the immunoexpression of HIF-1α, NOTCH1, ADAM12, and HB-EGF in cases of MEC. This may help elucidate specific cellular mechanisms involved in MEC behavior.

MATERIALS AND METHODS

Nineteen cases of MEC (Table I) and 10 samples of normal salivary glands were retrieved from the files of the Department of Oral Pathology at the School of Dentistry of University Center of Pará (CESUPA), Belém, Pará, Brazil. Histologic grading was performed according to the criteria proposed by Brandwein et al.[3] Ten samples of normal salivary glands were included as a control group. This study followed the guidelines of Helsinki Declaration and was approved by the Ethics Committee of the Institute of Health Sciences at Federal University of Pará (1.516.755).

Formalin-fixed, paraffin-embedded tissues were studied by using the immunoperoxidase technique. Four-micron sections were obtained and mounted on

Table II. Higher immunoexpression of HIF-1α in 19 MEC samples in comparison with the control group of salivary glands

MEC			*CG*			
Intensity of staining (%)	*Score*	*Localization*	*Intensity of staining (%)*	*Score*	*Localization*	P value
57.01	2		29.8	1		
60.05	2		4.6	1		
70.3	2		46.6	1		
74.3	2		38.2	1		
50.3	2		18.3	1		
33	1		29.6	1		
38.5	1		19.7	1		
31.5	1		42.7	1		
42.6	1		39.8	1		
80	2	Cytoplasmic and nuclear	35.4	1	Nonspecific	.0012*
59.2	2		–	–		
60.5	2		–	–		
42.5	1		–	–		
48.7	1		–	–		
65.1	2		–	–		
30.1	1		–	–		

(continued)

Table II. Continued

MEC			*CG*			
Intensity of staining (%)	*Score*	*Localization*	*Intensity of staining (%)*	*Score*	*Localization*	P value
45.2	1		–	–		
47.3	1		–	–		
33.1	1		–	–		

*Statistical significance: $P \leq .01$.
CG, control group; *MEC,* mucoepidermoid carcinoma.

Table III. Higher immunoexpression of NOTCH1 in 19 MEC samples in comparison with the control group of salivary glands.

MEC			*CG*			
Intensity of staining (%)	*Score*	*Localization*	*Intensity of staining (%)*	*Score*	*Localization*	*P value*
76.3	2		51.4	2		
24.9	1		39.2	1		
70.1	2		29.8	1		
65.2	2		32.6	1		
51.7	2		40.6	1		
67.0	2		40.7	1		
40.1	1		47.7	1		
80.8	2		34.2	1		
52.8	2		49.6	1		
44.8	1	Cytoplasmic and nuclear	44.1	1	Nonspecific	.0012*
68.0	2		–	–		
70.2	2		–	–		
55.3	2		–	–		
54.6	2		–	–		
60.9	2		–	–		
72.8	2		–	–		
66.1	2		–	–		
57.5	2		–	–		
71.1	2		–	–		

*Statistical significance: $P \leq .01$.
CG, control group; *MEC,* mucoepidermoid carcinoma.

Table IV. Higher immunoexpression of ADAM12 in 19 MEC samples in comparison with the control group of salivary glands.

MEC			*CG*			
Intensity of staining (%)	*Score*	*Localization*	*Intensity of staining (%)*	*Score*	*Localization*	*P value*
69.4	2		38.9	1		
63.9	2		30.4	1		
51.7	2		32	1		
66.9	2		40.4	1		
50.8	2		39.4	1		
52	2		45.4	1		
60.1	2		42.1	1		
67.3	2		32.9	1		
63	2		41.3	1		
70.7	2	Cytoplasmic and nuclear	34	1	Nonspecific	< .0001*
70	2		–	–		
66.9	2		–	–		
53.6	2		–	–		
61.9	2		–	–		
83.4	2		–	–		
57.2	2		–	–		
59.6	2		–	–		

(*continued*)

Table IV. Continued

MEC			*CG*			
Intensity of staining (%)	*Score*	*Localization*	*Intensity of staining (%)*	*Score*	*Localization*	*P value*
60.1	2		–	–		
62.3	2		–	–		

*Statistical significance: $P \leq .01$.
CG, control group; *MEC,* mucoepidermoid carcinoma.

Table V. Higher immunoexpression of HB-EGF in 19 MEC samples in comparison with the control group of salivary glands

MEC			*CG*			
Intensity of staining (%)	*Score*	*Localization*	*Intensity of staining (%)*	*Score*	*Localization*	*P value*
68.6	2		29.8	1		
65.9	2		4.6	1		
69.3	2		46.7	1		
58.9	2		38.2	1		
71.1	2		18.4	1		
82	2		29.6	1		
71	2		19.8	1		
84.5	2		42.8	1		
52.9	2		39.9	1		
72.5	2	Cytoplasmic and nuclear	35.4	1	Nonspecific	< .001*
77.9	2		–	–		
60.7	2		–	–		
66.9	2		–	–		
71	2		–	–		
68.9	2		–	–		
71.5	2		–	–		
46.1	1		–	–		
63.2	2		–	–		
69.7	2		–	–		

*Statistical significance: $P \leq .01$.
CG, control group; *MEC,* mucoepidermoid carcinoma.

poly-D-lysine-coated slides (Sigma-Aldrich, St. Louis, MO). Sections were dewaxed in xylene and rehydrated in a graded ethanol series. Antigen retrieval was carried out in a Pascal chamber (Dako, Carpinteria, CA) for 30 seconds. Sections were immersed in 3% hydrogen peroxide in methanol for 20 minutes to inhibit endogenous peroxidase activity and then blocked with 1% bovine serum albumin (BSA; Sigma, St. Louis, MO) in phosphate-buffered saline for 1 hour.

The samples were incubated with the following primary antibodies: anti-HIF-1α (1:50, rabbit; Millipore, Darmstadt, CA); anti-NOTCH1 (1:250, rabbit, Millipore, Darmstadt, CA); anti-ADAM-12 (1:50, goat; Bioss, Cambridge, MA), and anti-HBEGF (1:15, goat; R&D Systems, MN). All primary antibodies were diluted in antibody diluent solution (Dako, Carpinteria, CA) and incubated for 1 hour at room temperature. Subsequently, the slides were incubated for 30 minutes with the *EnVision Plus* (Dako, Carpinteria, CA) detection system. Diaminobenzidine (Sigma, St. Louis, MO) was used as a chromogen, and the sections were

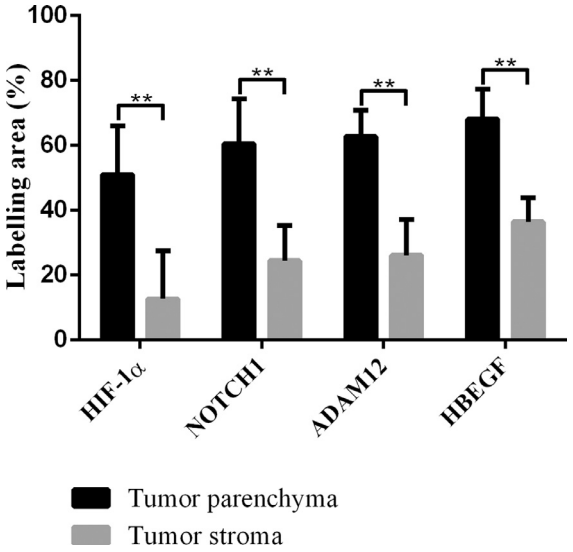

Fig. 1. Higher immunoexpression of HIF-1α, NOTCH1, ADAM-12, and heparin-binding endothelial growth factor–-like growth factor (HB-EGF) in tumor parenchyma in comparison with stroma of mucoepidermoid carcinoma (MEC). Statistical significance: ** $P \leq .01$.

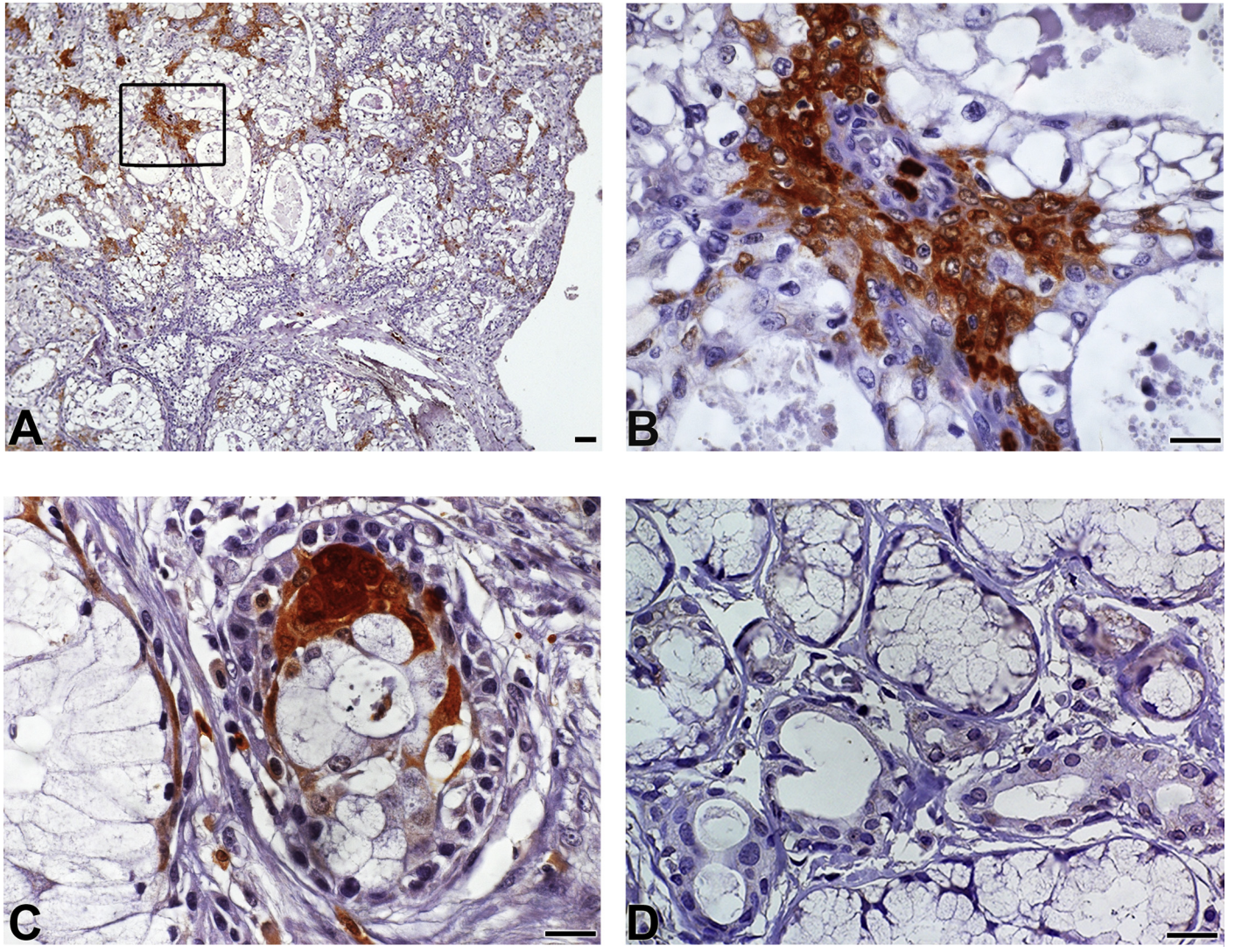

Fig. 2. HIF-1α immunoexpression in mucoepidermoid carcinoma (MEC) and control group (CG) samples. **A,** HIF-1α shows strong immunostaining in epidermoid cells of MEC, and the stroma was weakly stained. **B,** The cytoplasm and nuclei of epidermoid cells were strongly stained. **C,** Weakly stained mucous cells of MEC surrounding a cystic area. **D,** Immunostaining in secretory cells of CG (magnifications $\times$ 100 and $\times$ 630; scale bars: 50 and 20 μm). *A high-resolution version of this slide for use with the Virtual Microscope is available as eSlide: VM05303.*

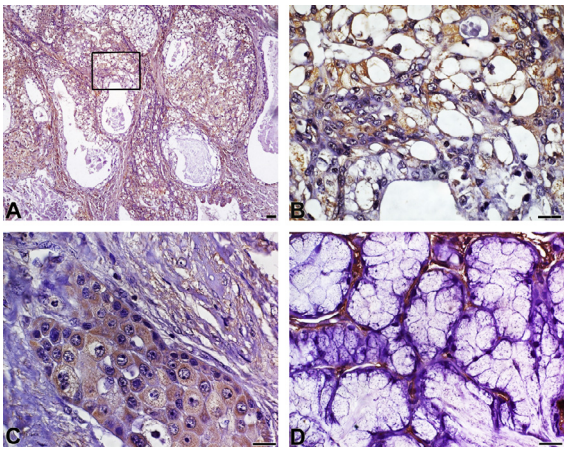

Fig. 3. NOTCH1 immunoexpression in mucoepidermoid carcinoma (MEC) and control group (CG) samples. **A,** NOTCH1 was strongly stained in epidermoid cells of MEC. **B,** Strong staining of the cytoplasm of epidermoid cells; mucous cells were weakly stained. **C,** Cytoplasmic immunoexpression in intermediate and epidermoid cells. **D,** Immunostaining located in glandular stroma of CG (magnifications × 100 and × 630; scale bars: 50 and 20 μm). *A high-resolution version of this slide for use with the Virtual Microscope is available as eSlide: VM05304.*

counterstained with Mayer hematoxylin (Sigma, St. Louis, MO). Finally, the samples were mounted in Permount.

Brightfield images from 10 randomly selected images from each sample were acquired by using an AxioScope 40 microscope (Carl Zeiss, Oberkochen, Germany) equipped with a charge-coupled device color camera. All images were acquired at the same magnification (× 400).

Immunoexpression analysis was carried out for HIF-1α, NOTCH1, ADAM12, and HB-EGF in the MEC and control groups. Areas of diaminobenzidine staining were separated and segmented by using the color deconvolution plug-in of ImageJ software (public domain; software developed by Wayne Rasband, MD), and the average percent labeled area (%) was calculated.

The immunoexpression intensity and distribution were evaluated according to the criteria proposed by Vasconcelos et al.[25] and adapted by us to determine the immunostaining in the parenchyma and stroma and the cellular localization of the staining (membrane, nucleus, and cytoplasm) in MEC cells. Staining intensity was classified into the following scores, according the percentage of labeled area: 0 = no staining; 1 = weak staining (<50% labeled cells); and 2 = strong staining (≥50% labeled cells). We considered greater than 10% of labeling cells as positive staining. We used our pattern of evaluation to define greater than 50% of labeling cells as strong intensity. The distribution was also quantitatively assessed as focal (<50% labeled cells) and diffuse (>50% labeled cells).

Data were analyzed by using GraphPad Prism 6.0 software (GraphPad Software, Inc., San Diego, CA). A significance level of 1% was applied ($P \leq .01$). The Student t test was performed to compare the immunoexpression of HIF-1α, NOTCH1, ADAM-12, and HB-EGF between the MEC and control groups, between the stroma and the tumor parenchyma, and between the mucous and epidermoid cells of MEC. Spearman's correlation test was performed for determining the correlation between the intensity of staining and the histopathologic grade[3,6] in the MEC cases.

RESULTS

HIF-1α, NOTCH1, ADAM-12, and HB-EGF were expressed in all samples of MEC (n = 19) and in the control group of normal salivary glands (n = 10). However, immunostaining was statistically more intense in the MEC samples than in the control group (Tables II-V).

The tumoral stroma of the MEC samples showed low, weak, and focal immunoexpression in comparison with the tumor parenchyma (Figure 1).

HIF-1α had a strong, diffuse immunoexpression (mean immunostaining 51%) in the nucleus and cytoplasm of the MEC parenchyma (Figures 2A to 2C). In the control group (Figure 2D), we found weak and focal expression for HIF-1α (mean 30.5%).

NOTCH1 showed a high intensity of staining and a diffuse distribution (mean 60.5%) located in the cytoplasm and nucleus of the epidermoid cells of the MEC parenchyma (Figures 3A to 3C). The control group (Figure 3D) presented weak staining intensity (mean 41%).

ADAM12 immunoexpression was strong, diffuse, and located in the cytoplasm and nucleus (Figures 4A to 4C) of epidermoid cells. ADAM12 showed staining intensity and distribution mean of 62.68%. The normal salivary glands samples showed weak and focal immunostaining (mean labeling area 37%) (Figure 4D).

Immunostaining of HB-EGF was strong, diffuse, cytoplasmic, and nuclear in epidermoid cells (Figures 5A to 5C) of tumor parenchyma (68%). The control group demonstrated weak staining (Figure 5D) (mean 30.5%).

Moreover, the proteins of interest exhibited intense and statistically higher ($P \leq .01$) immunoexpression in the epidermoid cells than in the mucous cells of the MEC cases (Figure 6).

There was no correlation between each protein of interest and the histopathologic grade of the MEC cases (Table VI).

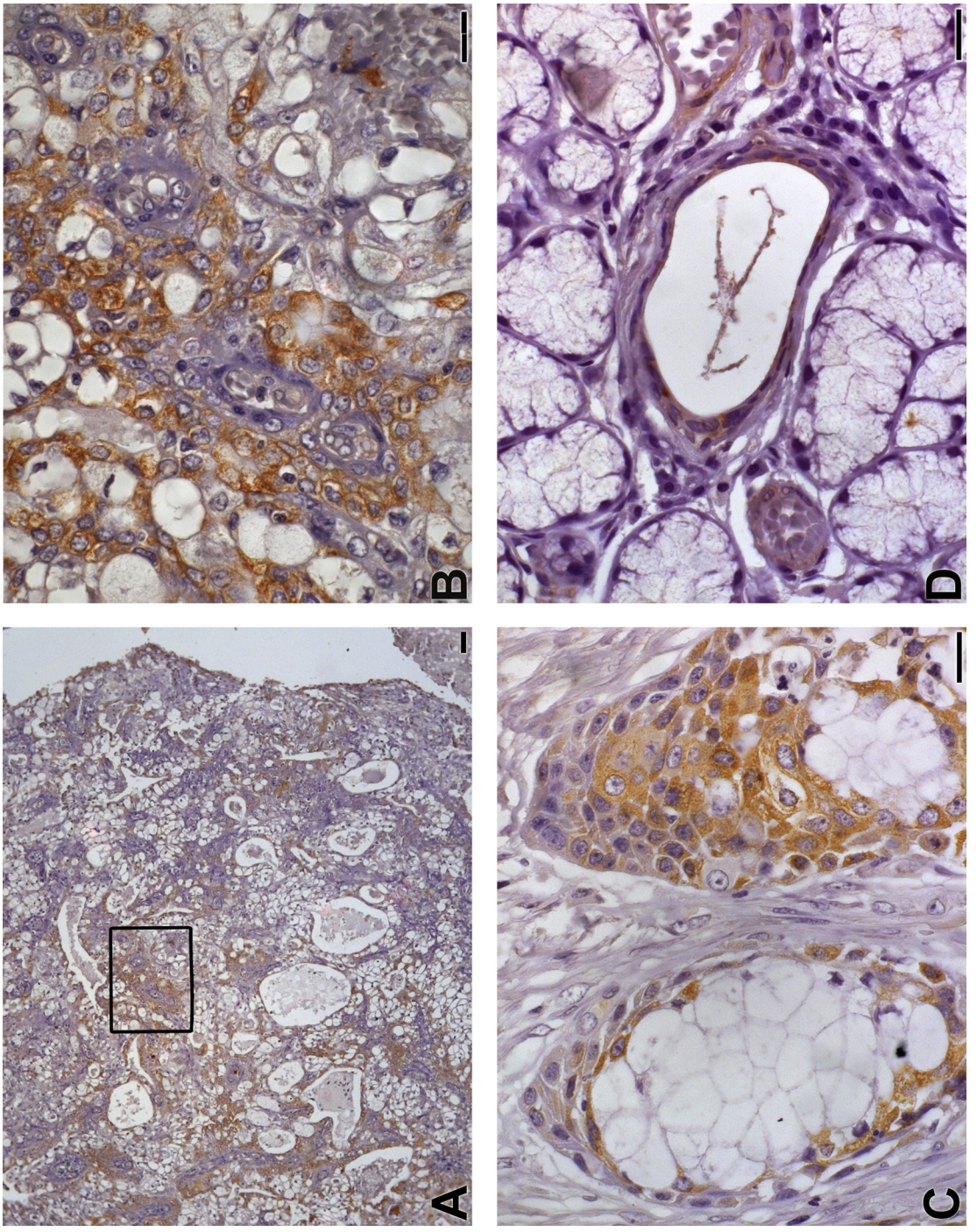

Fig. 4. ADAM12 immunoexpression in mucoepidermoid carcinoma (MEC) and control group (CG) samples. **A and B,** Immunoexpression was strong and uniform in the cytoplasm of epidermoid cells in MEC, and the stroma was weakly stained. **C,** Epidermoid cells with intensely stained cytoplasm surrounding mucous cells with low labeling intensity. **D,** Immunostaining in the glandular stroma and CG myoepithelial cells (magnifications × 100 and × 630; scale bars: 50 and 20 μm). *A high-resolution version of this slide for use with the Virtual Microscope is available as eSlide: VM05305.*

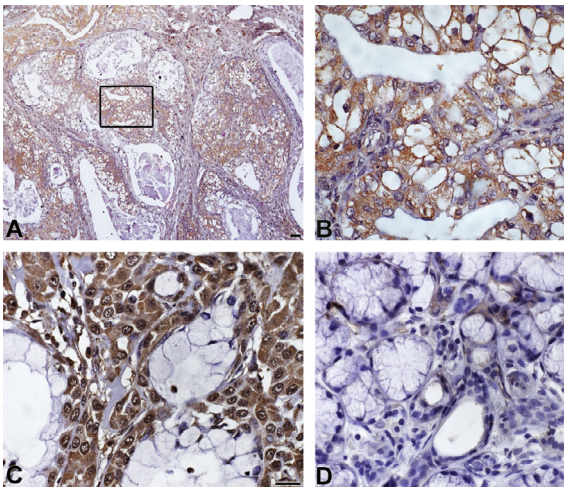

Fig. 5. Heparin-binding epidermal growth factor–like growth factor (HB-EGF) immunoexpression in mucoepidermoid carcinoma (MEC) and control group (CG) samples. **A and B,** Cytoplasm and nuclear immunostaining of epidermoid cells of MEC. **C,** Immunostaining of cytoplasm and nucleus of epidermoid cells and presence of mucous cells. D, Immunostaining located in glandular stroma of CG (magnifications × 100 and × 630; scale bars: 50 and 20 μm). *A high-resolution version of this slide for use with the Virtual Microscope is available as eSlide: VM05306.*

DISCUSSION

MEC is the most common malignant tumor of the salivary glands and exhibits varied biologic behavior, which makes therapy difficult.[3,6] Studies aimed at understanding the signaling pathways of the MEC pathologic processes deserve attention. Therefore, this original work described the immunoexpression of IH-related proteins in MEC samples; this has not been reported so far in the current literature. We observed higher immunostaining of HIF-1α, NOTCH1, ADAM12, and HB-EGF, mainly in the tumor epidermoid cells in comparison with stroma.

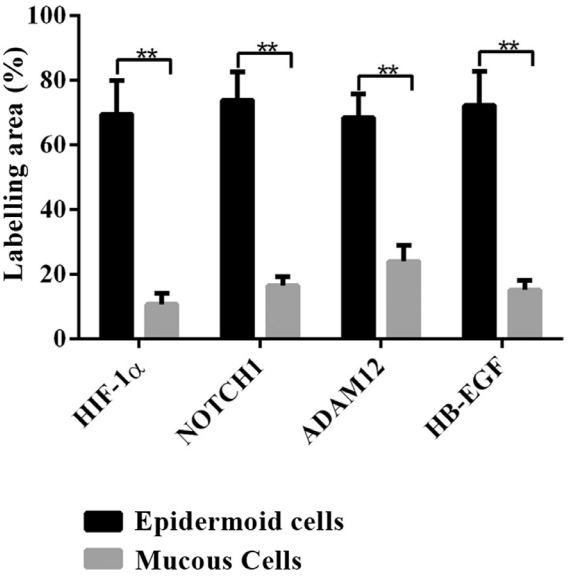

Fig. 6. Higher immunoexpression of HIF-1α, NOTCH1, ADAM-12, and heparin-binding epidermal growth factor–like growth factor (HB-EGF) in epidermoid cells in comparison with mucous cells of mucoepidermoid carcinoma (MEC). Statistical significance: ** $P \leq .01$.

We found strong nuclear and cytoplasmic expression of HIF-1α in the epidermoid cells. Stable expression of HIF-1α occurs in the nucleus, providing stabilization of the intracellular responses and transcription of several genes associated with cellular invasiveness.[12,20] HIF-1α exhibits classic nuclear localization but sometimes can be found expressed in the cytoplasm as a result of the saturation of proteins responsible for cytoplasmic HIF-1α degradation, which could result in high cytoplasmic levels of HIF-1α.[26]

Studies have associated the overexpression of HIF-1α with therapy resistance, poor prognosis, and aggressiveness of many malignant neoplasms.[27-29] Nevertheless, under hypoxic conditions, HIF-1α can induce the formation of invadopodia, which are finger-like cellular projections responsible for proteolysis located in the extracellular matrix.[30-33] This consequently increases extracellular matrix degradation, leading to tumor progression and metastasis.[33]

Stabilization of HIF-1α at low concentrations of O_2 increases the expression of Jagged-2 ligand, triggering NOTCH1 signaling.[34] Deregulation and overexpression of NOTCH1 has been verified in certain types of cancers.[35-37] Our findings showed strong cytoplasmic and punctate nuclear immunostaining of NOTCH1 in epidermoid cells. This could occur during NOTCH1 signaling, when the intracellular domain of NOTCH1 is cleaved and translocates to the nucleus. This process will regulate a series of events associated with cellular proliferation and differentiation.[19-21]

Among the proteins activated by NOTCH1 is ADAM12.[19] Our results confirmed strong immunostaining of ADAM12 in MEC, mainly in the cytoplasm of the epidermoid cells of the tumor parenchyma. This labeling pattern is consistent with that found in studies in breast carcinoma[33] and ameloblastoma.[38,39] ADAM12 is a metalloproteinase responsible for the cleavage of biologically active ligands from its ectodomains and is required for the formation of distant metastases because it contributes to the formation of invadopodia through the release of growth factors, such as HB-EGF.[23,38,39]

In this study, we observed overexpression of HB-EGF predominantly in the cytoplasm and occasionally in the nucleus of MEC epidermoid cells. The pattern of cytoplasmic labeling of HB-EGF coincides with the location of ADAM12 staining, which may be related to the role of this metalloproteinase in the cleavage and release of HB-EGF in MEC.

Table VI. Correlation between the staining intensity of HIF-1 α, NOTCH1, ADAM12, and HB-EGF and histopathologic grade of 19 MEC cases

	Variable				
	Histologic grade				
	Low	*High*	*Total*	*r*	*P value*
HIF-1 α					
Staining intensity				0.1	.6
Weak	4 (21.6)	3 (15.7)	7 (37.3)		
Strong	11 (57.5)	1 (5.2)	12 (62.7)		
NOTCH1					
Staining intensity				0.2	.3
Weak	2 (10,5)	1 (5.2)	3 (15.7)		
Strong	13 (68,4)	3 (15.7)	16 (84.3)		
ADAM12					
Staining intensity				0.1	.6
Weak	0	0	0		
Strong	15 (78.4)	4 (21.6)	19 (100)		
HB-EGF					
Staining intensity				0.1	.6
Weak	1 (5.2)	0	1 (5.2)		
Strong	15 (78.4)	3 (15.7)	18 (94.8)		

Data presented as n (%).
r = Correlation coefficient.
Statistical significance: $P \leq .01$.

In addition, the intracellular domain of ADAM12 can bind to TKs5. TKs5 is a key protein in the recruitment of actin filaments that compose invadopodia. That process shows the indirect influence of ADAM12 in the formation of invadopodia, which are primordial structures in the onset of neoplastic dissemination in both benign and malignant cases.[36,40]

In the analysis of the staining patterns of the proteins under study, we observed that all of them showed intense staining on epidermoid cells and poor labeling on the mucous cells of MEC. The predominance of the epidermoid cell type is one of the main characteristics of histopathologic grade III,[3] and it is related to lower survival rates and higher mortality.[4] Thus, the predilection of these proteins for epidermoid cells may be related to the greater aggressiveness of the MEC.

CONCLUSIONS

From these findings, we conclude that HIF-1α, NOTCH1, ADAM12, and HB-EGF proteins may be associated with the mechanisms of MEC invasion. The overexpression of these proteins demonstrates that neoplastic cells of the MEC are in IH, a condition that leads to the activation of the signaling pathway capable of inducing invadopodia formation through a cascade of cellular events studied in this work; thus, this cascade may contribute to greater invasiveness and aggressiveness of the tumor.

REFERENCES

1. Azevedo RS, Almeida OP, Kowalski LP, Pires FB. Comparative cytokeratin expression in the different cell types of salivary gland mucoepidermoid carcinoma. *Head Neck Pathol*. 2008;2:257-264.
2. Byrd SA, Spector ME, Carey TE, Bradford CR, McHugh JB. Predictors of recurrence and survival for head and neck mucoepidermoid carcinoma. *Otorhinolaryngol Head Neck Surg*. 2013;149:402-408.
3. Brandwein MS, Ivanov K, Wallace DI, et al. Mucoepidermoid carcinoma: a clinicopathologic study of 80 patients with special reference to histologic grading. *Am J Surg Pathol*. 2001;25:835-845.
4. Coca-Pelaz A, Rodrigo JP, Triantafyllou A, et al. Salivary mucoepidermoid carcinoma revisited. *Eur Arch Otorhinolaryngol*. 2015;272:799-819.
5. Luna MA. Salivary mucoepidermoid carcinoma: revisited. *Adv Anat Pathol*. 2006;13:293-307.
6. Nance MA, Seethala RR, Wang Y, et al. Treatment and survival outcomes based on histologic grading in patients with head and neck mucoepidermoid carcinoma. *Cancer*. 2008;113:2082-2089.
7. Wijffels KI, Hoogsteen IJ, Lok J, et al. No detectable hypoxia in malignant salivary gland tumors: Preliminary results. *Int J Radiat Oncol Biol Phys*. 2008;71:1319-1325.
8. Ishibashi H, Shiratuchi T, Nakagawa K, et al. Hypoxia-induced angiogenesis of cultured human salivary gland carcinoma cells enhances vascular endothelial growth factor production and basic fibroblast growth factor release. *Oral Oncol*. 2001;37:77-83.
9. Walsh JC, Lebedev A, Aten E, Madsen K, Marciano L, Kolb HC. The clinical importance of assessing tumor hypoxia: relationship of tumor hypoxia to prognosis and therapeutic opportunities. *Antioxid Redox Signal*. 2014;21:1517-1541.
10. McKeown SR. Defining normoxia, physoxia and hypoxia in tumours—implications for treatment response. *Br J Radiol*. 2014;87:1-12.

11. Mimeault M, Batra SK. Hypoxia-inducing factors as master regulators of stemness properties and altered metabolism of cancer- and metastasis-initiating cells. *J Cell Mol Med*. 2013;17:30-54.
12. Brahimi-Horn MC, Chiche J, Pouyssegur J. Hypoxia and cancer. *J Mol Med*. 2007;85:1301-1307.
13. Marcu LG, Phillips WMH, Filip SM. Hypoxia in head and neck cancer in theory and practice: a PET-based imaging approach. *Comput Math Method Med*. 2014;13:1-13.
14. Chen J, Imanaka N, Chen J, Griffin JD. Hypoxia potentiates Notch signaling in breast cancer leading to decreased E-cadherin expression and increased cell migration and invasion. *Br J Cancer*. 2010;102:351-360.
15. Du Z, Fujiyama C, Chen Y, Masaki Z. Expression of hypoxia-inducible factor 1 alpha in human normal, benign, and malignant prostate tissue. *Chin Med J*. 2003;116:1936-1939.
16. Naruse T, Kawasaki G, Yanamoto S, Mizuno A, Umeda M. Immunohistochemical study of VEGF expression in oral squamous cell carcinomas: Correlation with the mTOR-HIF-1 alpha pathway. *Anticancer Res*. 2011;31:4429-4437.
17. Bai S, Chen H, Zhang Y, et al. Pien Tze Huang inhibits hypoxia-induced angiogenesis *via* HIF-1 alpha /VEGF-A pathway in colorectal cancer. *Evid Based Complement Alternat Med*. 2015. (2015:454279.
18. Bedogni B, Warneke JA, Nickoloff BJ, Giaccia AJ, Powell MB. NOTCH1 is an effector of Akt and hypoxia in melanoma development. *J Clin Invest*. 2008;118:3660-3670.
19. Díaz B, Yuen A, Iizuka S, Higashiyama S, Courtneidge SA. Notch increases the shedding of HB-EGF by ADAM12 to potentiate invadopodia formation in hypoxia. *J Cell Biol*. 2013;201:279-292.
20. Kadesch T. Notch signaling: the demise of elegant simplicity. *Curr Opin Genet Dev*. 2004;14:506-512.
21. Li H, Solomon E, Duhachek SM, Sun D, Zolkiewska A. Metalloprotease-disintegrin ADAM12 expression is regulated by Notch signaling *via* microRNA-29. *J Biol Chem*. 2011;286:21500-21510.
22. Kveiborg M, Albrechtsen R, Couchman JR, Wewer UM. Cellular roles of ADAM12 in health and disease. *Int J Biochem Cell Biol*. 2008;40:1685-1702.
23. Dateoka S, Ohnishi Y, Kakudo K. Effects of CRM197, a specific inhibitor of HB-EGF, in oral cancer. *Med Mol Morphol*. 2012;45:91-97.
24. Ohnishi Y, Inoue H, Furukawa M, Kakudo K, Nozaki M. Heparin-binding epidermal growth factor-like growth factor is a potent regulator of invasion activity in oral squamous cell carcinoma. *Oncol Rep*. 2012;27:954-958.
25. Vasconcelos MG, Vasconcelos 1, RG, Pereira de Oliveira DH, et al. Distribution of hypoxia-inducible factor-1 αand glucose transporter-1 in human tongue cancer. *J Oral Maxillofac Surg*. 2015;73:1753-1760.
26. Hagg M, Wennstrom S. Activation of hypoxia-induced transcription in normoxia. *Exp Cell Response*. 2005;306:180-191.
27. Goscinski MA, et al. Primary tumor vascularity in esophagus cancer. CD34 and HIF1-αexpression correlate with tumor progression. *Histol Histopathol*. 2013;28:1361-1368.
28. Sun G, Hu W, Lu Y, Wang Y. A meta-analysis of HIF-1 αand esophageal squamous cell carcinoma (ESCC) risk. *Pathol Oncol Res*. 2013;19:685-693.
29. Strauss E, Waliszewski K, Oszkinis G, Staniszewski R. Polymorphisms of genes involved in the hypoxia signaling pathway and the development of abdominal aortic aneurysms or large-artery atherosclerosis. *J Vasc Surg*. 2015;61:1105-1113.
30. Wang Y, Roche O, Xu C, et al. Hypoxia promotes ligand-independent EGF receptor signaling *via* hypoxia-inducible factor−mediated upregulation of caveolin-1. *Proc Natl Acad Sci U S A*. 2012;109:4892-4897.
31. Hanna SC, Krishnan B, Bailey ST, et al. HIF-1 α and HIF-2 α independently activate SRC to promote melanoma metastases. *J Clin Invest*. 2013;123:2078-2093.
32. Linder S, Wiesner C, Himmel C. Degrading devices: invadosomes in proteolytic cell invasion. *Annu Rev Cell Dev Biol*. 2011;27:185-211.
33. Hashin NF, Nicholas NS, Dart AE, Kiriakidis S, Paleogol E, Wells CM. Hypoxia-induced invadopodia formation: a role for β-PIX. *Open Biol*. 2013;6:1-10.
34. Pietras A, Von Stendingk K, Lindgren D, Pahlman S, Axelson H. JAG2 induction in hypoxic tumor cells alter NOTCH signaling and enhance endothelial cell tube formation. *Mol Cancer Res*. 2011;9:626-636.
35. Yoshida R, Nagata M, Nakayama H, et al. The pathologic significance of NOTCH1 in oral squamous cell carcinoma. *Lab Invest*. 2013;93:1068-1081.
36. Courtneidge SA, Azucena EF, Pass I, Seals DF, Tesfav L. The SRC substrate Tks5, podosomes (invadopodia), and cancer cell invasion. *Cold Spring Harb Symp Quant Biol*. 2005;70:167-171.
37. Frohlich C, Klitgaard M, Noer JB, et al. ADAM12 is expressed in the tumour vasculature and mediates ectodomain shedding of several membrane-anchored endothelial proteins. *Biochem J*. 2013;452:97-109.
38. Lendeckel U, Kohl J, Arndt M, Carl-McGrath S, Donat H, Rocken C. Increased expression of ADAM family members in human breast cancer and breast cancer cell lines. *J Cancer Res Clin Oncol*. 2005;131:41-48.
39. Paz H, Pathak N, Yang J. Invading one step at a time: the role of invadopodia in tumor metastasis. *Oncogen J*. 2014;14:4193-4202.
40. da Costa NMM, Fialho ADV, Proietti CC, et al. Role of hypoxia-related proteins in invasion of ameloblastoma cells: cross talk between NOTCH1, hypoxia-inducible factor 1 α, a disintegrin and metalloproteinase 12, and heparin-binding epidermal growth factor. *Histopathol*. 2016;69:99-106.

Reprint requests:

Dimitra Castelo Branco, Federal University of Pará, Institute of Health Sciences, School of Dentistry, Avenida Augusto Corrêa, 01. Belém PA, 66075-110, Brazil.
Dimitra.castelo@gmail.com